https://doi.org/10.15407/ufm.25.03.520

V.A. DEKHTYARENKO [1,2,*], T.V. PRYADKO [1,], T.P. VLADIMIROVA [1,***], S.V. MAKSYMOVA [2], H.Yu. MYKHAILOVA [1], and V.I. BONDARCHUK [1]**

[1] G.V. Kurdyumov Institute for Metal Physics of the N.A.S. of Ukraine, 36 Academician Vernadsky Blvd., UA-03142 Kyiv, Ukraine

[2] E.O. Paton Electric Welding Institute of the N.A.S. of Ukraine, 11 Kazymyr Malevych Str., UA-03150 Kyiv, Ukraine

* devova@i.ua, ** pryadko@imp.kiev.ua, *** tvlad@imp.kiev.ua

EFFECT OF ALLOYING ON THE HYDROGEN SORPTION IN Ti–Zr–Mn-BASED ALLOYS. Pt. 1: *C*14-Type Laves-Phase-Based Alloys

The alloys of the Ti–Zr–Mn system based on the *C*14-type Laves phase are considered as ones of the most promising materials for safe storage and transportation of hydrogen. These alloys have appropriate parameters for activating the processes of absorption and release of hydrogen, a low cost, and a fairly high cyclic stability. In this work, the microstructure and phase composition of the starting alloys and the crystal structure of the hydrides synthesized from them are studied. Possible ways to reduce the cost of the final products are shown. The fact that changing the method of the alloy fabrication does not significantly affect its hydrogen absorption properties is shown. On the example of the considered alloys, it is shown that, as expected, alloying with an element with a larger atomic radius that forms a stable chemical compound with hydrogen results in an increase in the hydrogen capacity. This is explained by both the increased radius of the tetrahedral interstitial sites, where hydrogen atoms are located after dissolution, and the higher total amount of the element interacting with hydrogen..

Keywords: Laves phase, intermetallic compound, alloying element, tetrahedral interstitial sites, hydrogenation–dehydrogenation, hydrogen capacity.

1. Introduction

Since the end of the 70th of the last century [1–5] and until now [6–10], AB_2-type intermetallic compounds (alloys based on the Laves phase) are considered the most promising materials for storing and transporting hydrogen. There are many intermetallic compounds of this type that can be

Citation: V.A. Dekhtyarenko, T.V. Pryadko, T.P. Vladimirova, S.V. Maksymova, H.Yu. Mykhailova, and V.I. Bondarchuk, Effect of Alloying on the Hydrogen Sorption in Ti–Zr–Mn-Based Alloys. Pt. 1: *C*14-Type Laves-Phase-Based Alloys, *Progress in Physics of Metals*, **25**, No. 3: 520–544 (2024)

used for hydrogen accumulation; however, the $TiMn_2$ compound is a special one [11–13]. This is explained by comparatively simple activation of the hydrogenation [14], rather significant hydrogen capacity (≈1.0 H/*Me* [15], where H/*Me* denotes the hydrogen-to-metal host atom ratio), and a high rate of interaction with hydrogen [16]. In addition, this compound has a fairly wide range of homogeneity (30–41 at.% Ti) [17, 18]. In Refs. [17, 19], it was noted that the hydrogen-sorption properties of the alloys based on $TiMn_2$ intermetallic compounds largely depend on their chemical composition. The authors of Ref. [17] showed that the best properties (at such hydrogenation parameters as a hydrogen pressure of 3.2 MPa and room temperature) had the alloys with composition which corresponded to the lower limit of the homogeneity region of the $TiMn_2$ intermetallic compound (*i.e.*, with the maximum titanium content). At the same time, the alloys with the maximum manganese content did not interact with hydrogen at all.

In addition, the $TiMn_2$ intermetallic compounds are superior to other intermetallic compounds (*e.g.*, $LaNi_5$) [20] which are used in autonomous hydrogen sources, due to their low specific gravity [21], which is especially important for vehicle batteries. At the same time, the main disadvantages of $TiMn_2$-based alloys are a high equilibrium pressure plateau and the hysteresis effect [22], which limits their practical application. Despite there were attempts to improve hydrogen-sorption properties by sorption–desorption cycling, the authors of Ref. [23] concluded that these properties could only be improved by alloying.

Partial substitution of titanium with zirconium (as the component *A*) was suggested in Ref. [24]. Based on the concept proposed in [23, 24], we proposed a new composition $(Ti_{0.34}Zr_{0.66})Mn_{1.2}$ [25] with the *C*14-type Laves phase with the $P6_3/mmc$ space group ($MgZn_2$ structure), which had better hydrogen-sorption properties as compared to existing analogues. The authors of Ref. [25] showed that, due to the partial substitution of titanium with zirconium, it was possible to expand the field of existence of the *C*14-type Laves phase up to 54.4 at.% Mn, and this, in turn, allowed increasing the hydrogen capacity up to H/*Me* = 1.2 and reducing the hydrogenation pressure from 3.2 MPa [17] to 0.60 MPa (at room temperature). This enhancement of hydrogen-sorption properties is explained by a higher affinity for hydrogen of zirconium as compared to titanium. In addition, zirconium has a larger atomic radius (0.160 nm) compared to titanium (0.147 nm), so, the lattice constants increase when titanium atoms are partially substituted by zirconium ones. This results in an increase in the radius of the tetrahedral interstitial sites in the lattice, which are potential sites for absorbed hydrogen atoms; this provides more space for hydrogen atoms, which increases hydrogen capacity. Furthermore, the total amount of an element readily interacting with hydrogen increases in the alloy [26]. However, the ever-increasing requirements for hydrogen

battery materials (operating time of hydrogen battery without recharging) require the development of new alloys or improvement of existing ones. That is why the developed $(Ti_{0.34}Zr_{0.66})Mn_{1.2}$ alloy was taken as the basis for our development of a series of new compositions with enhanced hydrogen-sorption–desorption kinetics and increased hydrogen capacity. Based on the literature [27], we used the alloying method as the most effective among other ones with the aim to improve the developed $(Ti_{0.34}Zr_{0.66})Mn_{1.2}$ alloy. Vanadium, chromium, nickel and cobalt were selected as alloying elements.

These alloying elements were selected for the following reasons. These elements readily interact with hydrogen [28–32], and they are relatively cheap as compared to other hydride-forming metals (*e.g.*, REMs). In addition, these elements form the *C*14-type Laves phase of with titanium and zirconium [33–36]. Besides, addition of these elements with larger atomic radii compared to manganese (vanadium and chromium) leads to an increase in the lattice constants and, accordingly, to an increase in the size of the interstitial sites, which should result in higher hydrogen capacity. Another reason for reducing Mn content in the alloy (while preserving its phase composition) is the melting temperature of this element (1246 °C, which is lower by more than 400 °C compared to other components). A significant difference in the melting temperatures between manganese and other alloying elements leads to the burning-out of Mn during the production of the alloy. This results in significant technological difficulties and increases the cost of the alloy due to the need for an additional 4.0 wt.% Mn [37] to achieve the target composition. In addition, the Mn burning-out harms the environment.

The concentration limits of alloying with the above-mentioned elements were chosen based on the literature [38]. In Ref. [38], the hydrogen-sorption properties of alloys of the Ti–V system were studied. It was shown that, in the range of vanadium concentrations of 0.25–5.0 at.%, it was possible to form hydride with an increased hydrogen content H/*Me* = 2.18.

2. Alloying-Caused Structural and Phase-Composition Changes

To determine the effect of alloying on the hydrogen-sorption properties of the $(Ti_{0.34}Zr_{0.66})Mn_{1.2}$ alloy, manganese was partially substituted by 5 at.% of each of the above-mentioned elements. The compositions of the compared alloys are listed in Table 1. In order to reveal the possibility of reducing the cost of hydride by the replacement of highly pure (and expensive) components with cheaper ones, an alloy $(Ti_{0.34}Zr_{0.66})Mn_{0.96}V_{0.12}Cr_{0.11}$ was also smelted using titanium of various grades for the charge [39]. High-purity iodide titanium (contained 0.02% Al, 0.02% Fe, 0.01% Si, 0.01% Mo, 0.005% Mn, 0.01% Ni, 0.01%, and trace amount of Cr, C, O, N) cost of

1800 UAH/kg and a TG-110 titanium sponge with a significantly higher content of impurities (0.09% Fe, 0.02% Si, 0.04% Ni, 0.05% O, 0.03% C, 0.02% N, 0.08% Cl) cost of 200–250 UAH/kg were used.

The samples with mass up to 30 grams were smelted in a KPTM-2 laboratory electric-arc furnace with a non-consumable tungsten electrode on a water-cooled copper base in a purified argon atmosphere [25, 39–42]. The vacuum system provided the pressure in the melting chamber at the level of $2.67 \cdot 10^{-3}$ Pa, and then, the chamber was filled with inert gas (argon). The maximum pressure of inert gas was $5.1 \cdot 10^{4}$ Pa. The furnace had a power of 15 kW at an arc voltage of 30 V and a current of 500 A. The arc was powered by a standard rectifier VDU-504. The charge was remelted up to 5 times to achieve high homogenization of the ingots. The following components were used for the charge: iodide Ti — 99.95 [25, 40, 41] or titanium sponge (TG-110) [39, 42–44]; iodide Zr — 99.975; electrolytic Mn — 99.9; electrolytic V — 99.5; electrolytic Cr — 99.9; electrolytic Ni — 99.5; and finally electrolytic Co — 99.5.

The practical application of hydrogen storage materials requires the development of relatively cheap techniques for producing ingots of various shapes and sizes in large amounts. Most of the alloys listed in Table 1 were produced as laboratory ingots (with weights up to 30 g) melted by the technique of electric-arc melting [25, 39–41, 43]. In order to evaluate the possibility of producing heavier ingots by various smelting techniques, an experimental $(Ti_{0.34}Zr_{0.66})Mn_{0.96}V_{0.12}Cr_{0.11}$ [42] ingot with a weight of up to 1 kg was produced by induction melting in an atmosphere of purified argon using open Al_2O_3 crucibles. This was done because, according to the literature [45–48], a change of the smelting technique can lead to either enhancement or deterioration of the hydrogen absorption properties.

Special technological conditions were proposed in Ref. [42], which ensured the complete remelting of components with significantly different melting points. Manganese was placed at the bottom of the crucible. This element has the lowest melting point, so it melted first and formed a liquid bath for all other components of the charge. Chromium was placed above manganese, as it has a lower density in the solid state and can float

Table 1. **Nominal compositions of alloys**

Formula	Alloy composition, at.%						
	Ti	Zr	Mn	V	Cr	Ni	Co
$(Ti_{0.34}Zr_{0.66})Mn_{1.2}$ [25]	15.4	30.2	54.4	—	—	—	—
$(Ti_{0.34}Zr_{0.66})Mn_{1.1}V_{0.1}$ [40]	15.4	30.2	49	5.4	—	—	—
$(Ti_{0.34}Zr_{0.66})Mn_{0.96}V_{0.12}Cr_{0.11}$ [39, 41, 42]	15.4	30.2	44	5.4	5	—	—
$(Ti_{0.34}Zr_{0.66})Mn_{0.86}V_{0.12}Cr_{0.11}Ni_{0.11}$ [43]	15.4	30.2	39	5.4	5	5	—
$(Ti_{0.34}Zr_{0.66})Mn_{0.84}V_{0.12}Cr_{0.12}Co_{0.12}$ [44]	15.5	30	38	5.5	5.5	—	5.5

up to the surface of the melt during melting. To avoid this, V was placed above Cr since the latter has a slightly higher melting point and, being in the solid state for a longer time, prevents chromium from floating. Titanium and zirconium were placed in the upper layer of the charge. They were the most active metals in the charge and therefore had to be in the liquid state for a shorter time to minimize the time of contact between their melt and the crucible.

Using scanning electron microscopy and x-ray phase analysis, the author of [42] proved that changing the smelting technology or increasing the ingot weight did not lead to the formation of new phases. The lattice constants of Laves phases coincided within the measurement error with the constants of the alloy produced by the electric arc technique [39]. This was also confirmed *via* the energy dispersive x-ray (EDX) analysis: the developed smelting scheme allowed preventing noticeable interaction between the melt and the crucible, so, aluminium from the crucible did not get into the ingot. It was also shown that the partial substitution of manganese (melting point 1246 °C) by vanadium and chromium (melting points 1910 and 1907 °C, respectively) reduced Mn losses caused by its burning-out. Therefore, the cost of the final product was also reduced.

The technology for producing massive ingots [42] was tested in Ref. [44] to produce multicomponent $(Ti_{0.34}Zr_{0.66})Mn_{0.84}V_{0.12}Cr_{0.12}Co_{0.12}$ alloy.

In Refs. [39–44], the phase compositions of the starting alloys and subsequent hydrides were determined using an automated DRON-3M diffractometer. CoK_α and CuK_α radiations were used, and the detector was

Table 2. **Lattice constants of phases in the as-cast state**

Alloys	Lattice constants ±0.0009, nm			
	l-phase *C*14	l-phase *C*15	Intermetallic compound Zr_2Ni	Intermetallic compound Zr_2Co
$(Ti_{0.34}Zr_{0.66})Mn_{1.2}$ [25]	a = 0.5051 c = 0.8297	—	—	—
$(Ti_{0.34}Zr_{0.66})Mn_{1.1}V_{0.1}$ [40]	a = 0.5064 c = 0.8318	—	—	—
$(Ti_{0.34}Zr_{0.66})Mn_{0.96}V_{0.12}Cr_{0.11}$ (titanium sponge) [39]	a = 0.5073 c = 0.8334	a = 0.7203	—	—
$(Ti_{0.34}Zr_{0.66})Mn_{0.86}V_{0.12}Cr_{0.11}Ni_{0.11}$ [43]	a = 0.5079 c = 0.8344	—	a = 1.2007	—
$(Ti_{0.34}Zr_{0.66})Mn_{0.96}V_{0.12}Cr_{0.11}$ (iodide titanium) [41]	a = 0.5093 c = 0.8372	a = 0.7188	—	—
$(Ti_{0.34}Zr_{0.66})Mn_{0.84}V_{0.12}Cr_{0.12}Co_{0.12}$ [44]	a = 0.5040 c = 0.8302	—	—	a = 1.1907

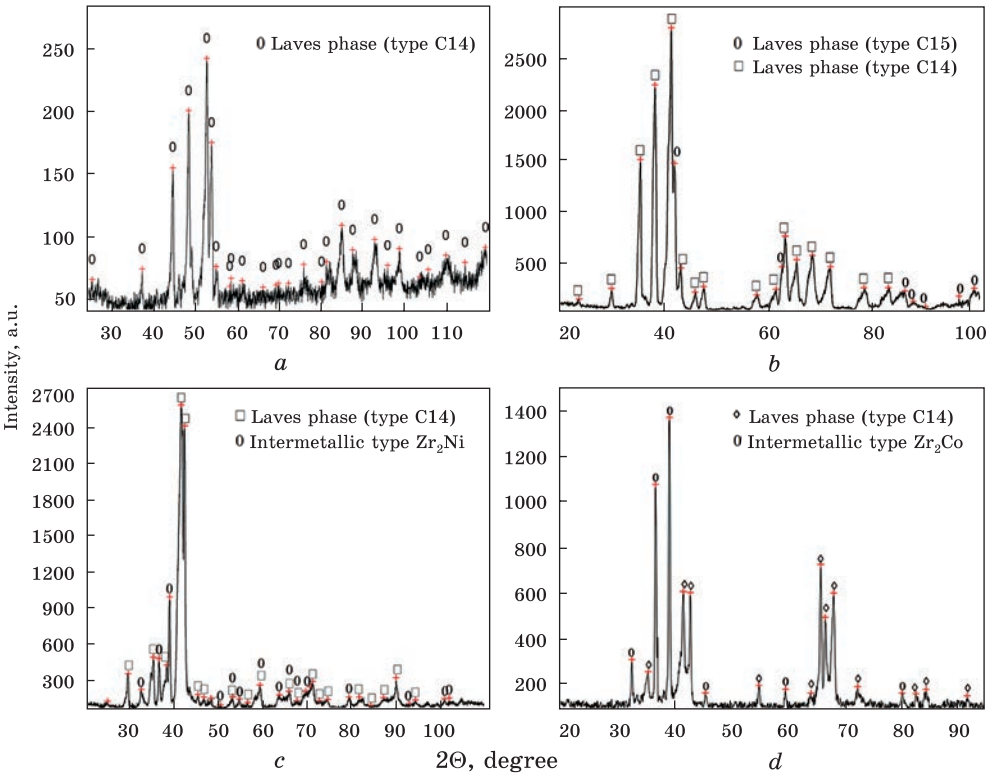

Fig. 1. Diffractograms of as-cast alloys: *a* — $(Ti_{0.34}Zr_{0.66})Mn_{1.2}$ [25] and $(Ti_{0.34}Zr_{0.66})Mn_{1.1}V_{0.1}$ [40]; *b* — $(Ti_{0.34}Zr_{0.66})Mn_{0.96}V_{0.12}Cr_{0.11}$ [39, 41, 42]; *c* — $(Ti_{0.34}Zr_{0.66})Mn_{0.86}V_{0.12}Cr_{0.11}Ni_{0.11}$ [43]; *d* — $(Ti_{0.34}Zr_{0.66})Mn_{0.84}V_{0.12}Cr_{0.12}Co_{0.12}$ [44]

moved with a step of 0.02°. The diffractograms were analysed using the RIR and Rietveld software package.

According to Ref. [40], the complete substitution of manganese with vanadium does not lead to changes in the phase composition of the $(Ti_{0.34}Zr_{0.66})Mn_{1.1}V_{0.1}$ alloy (Table 2, Fig. 1, *a*). At the same time, partial substitution of Mn with V, Cr, and Ni or Co results in changes in the phase composition, regardless of the titanium grade used in the charge [39, 41–44] (Table 2, Figs. 1, *b*–*d*).

According to Refs. [39, 41, 42], *C*15-type Laves phase (Fig. 1, *b*) with an f.c.c. lattice of the *Fd*3*m* space group ($MgCu_2$ structure) formed in the $(Ti_{0.34}Zr_{0.66})Mn_{0.96}V_{0.12}Cr_{0.11}$ alloy, in addition to *C*14-type hexagonal Laves phase of the $P6_3/mmc$ space group ($MgZn_2$ structure). In the alloys of $(Ti_{0.34}Zr_{0.66})Mn_{0.86}V_{0.12}Cr_{0.11}Ni_{0.11}$ [43] and $(Ti_{0.34}Zr_{0.66})Mn_{0.84}V_{0.12}Cr_{0.12}Co_{0.12}$ [44], the second phase was an intermetallic compound based on Zr_2Ni or Zr_2Co (Figs. 1, *c* and *d*) with an f.c.c. lattice of the *Fd*3*m* space group (Ti_2Ni structure).

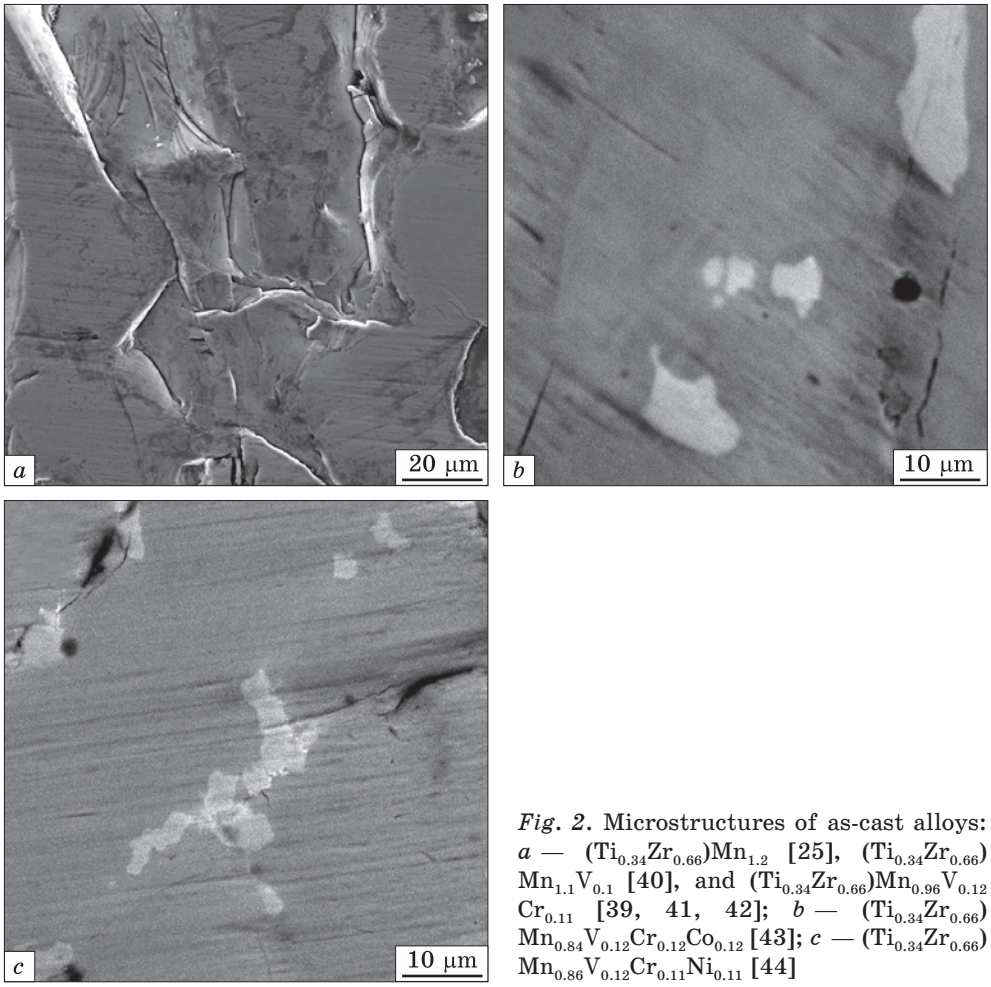

Fig. 2. Microstructures of as-cast alloys: *a* — $(Ti_{0.34}Zr_{0.66})Mn_{1.2}$ [25], $(Ti_{0.34}Zr_{0.66})Mn_{1.1}V_{0.1}$ [40], and $(Ti_{0.34}Zr_{0.66})Mn_{0.96}V_{0.12}Cr_{0.11}$ [39, 41, 42]; *b* — $(Ti_{0.34}Zr_{0.66})Mn_{0.84}V_{0.12}Cr_{0.12}Co_{0.12}$ [43]; *c* — $(Ti_{0.34}Zr_{0.66})Mn_{0.86}V_{0.12}Cr_{0.11}Ni_{0.11}$ [44]

There were no noticeable changes in the structure of the initial $(Ti_{0.34}Zr_{0.66})Mn_{1.2}$ alloy when Mn was partially substituted by Cr or V [39–42] (Fig. 2, *a*). Similarly to the $(Ti_{0.34}Zr_{0.66})Mn_{1.2}$ alloy, the structure of modified alloys consisted of coarse crystallites of the Laves phase (Table 1). At the same time, crystallites of the second phase were observed in the structure of the alloy, when manganese was partially substituted by three elements (vanadium, chromium, and nickel or cobalt) at once [43, 44] (Figs. 2, *b* and *c*).

According to the results of EDX analysis [43, 44], the dark crystallites (Figs. 2, *b* and *c*) correspond to the *C*14-type Laves phase (Table 3) with compositions of $(Ti_{0.29}Zr_{0.71})Mn_{1.22}V_{0.19}Cr_{0.16}Ni_{0.07}$ and $(Ti_{0.27}Zr_{0.73})Mn_{1.24}V_{0.17}Cr_{0.22}Co_{0.11}$. Unlike Cr and V, only a part of Co or Ni dissolves in the $(Ti_{0.34}Zr_{0.66})Mn_{1.2}$ alloy (*C*14-type Laves phase).

The authors of Refs. [39, 42, 43] explained the formation of the f.c.c.-*C*15-type Laves phase in the $(Ti_{0.34}Zr_{0.66})Mn_{0.96}V_{0.12}Cr_{0.11}$ alloy at such low Cr content as 5.0 at.%, basing on the Zr–Cr binary system phase diagram [49]. According to this diagram, two polymorphic transformations occur in this alloy during the solidification and cooling of the $ZrCr_2$ intermetallic compound (Laves phase). High-temperature γ-phase forms from the melt; then this phase transforms at 1622 °C into intermediate-temperature β-phase (*C*14-type Laves phase). The *C*14-type Laves phase persists to 1550 °C. At this temperature, the second phase transformation occurs: the α-phase (*C*15-type Laves phase) forms, which exists in equilibrium conditions at room temperature.

According to Refs. [43, 44], the presence of the second phase in alloys $(Ti_{0.29}Zr_{0.71})Mn_{1.22}V_{0.19}Cr_{0.16}Ni_{0.07}$ and $(Ti_{0.27}Zr_{0.73})Mn_{1.24}V_{0.17}Cr_{0.22}Co_{0.11}$ is explained by the impossibility of expanding the homogeneity region of the *C*14-type Laves phase below 44 at.% Mn with the methods used for alloy production. This suggestion was made based on the amount of manganese (Table 3) in the crystallites of the *C*14-type Laves phase. The volume fractions of the phases were determined [43, 44] using the free ImageJ software. This made it possible to determine how the presence of the second phase affects the main hydrogen-sorption characteristics of the alloys based on $(Ti_{0.34}Zr_{0.66})Mn_{1.2}$ composition [25]. As noted in Refs. [43, 44], the above-mentioned phases can significantly differ in hydrogenation-dehydrogenation parameters and hydrogen capacity. The volume fractions of the *C*14-type Laves phase (dark crystallites) in $(Ti_{0.29}Zr_{0.71})Mn_{1.22}V_{0.19}Cr_{0.16}Ni_{0.07}$ and $(Ti_{0.27}Zr_{0.73})Mn_{1.24}V_{0.17}Cr_{0.22}Co_{0.11}$ were 84.9 and 82.6%, respectively.

With aim to correctly determine the changes that occurred in the unit cell of the *C*14-type Laves phase in the $(Ti_{0.34}Zr_{0.66})Mn_{1.2}$ alloy alloyed with the above-mentioned elements [39–44], the volumes of the unit cell and the radii of the tetrahedral interstitial sites were calculated basing on the data of x-ray phase analysis (Table 2) (see Refs. [50–53]). As shown in Ref. [50], dissolved hydrogen atoms occupy tetrahedral interstitial sites regardless of the type of crystal lattice of the Laves phase. As authors [50–52] showed, the radius of the tetrahedral interstitial site can be calculated using the hard-sphere approximation as $R_s(C14) = 0.074475a$ and

Table 3. **The composition of phases (see Fig. 2) [43, 44]**

Alloys	Crystallites	Composition, at.%						
		Ti	Zr	Mn	V	Cr	Ni	Co
$(Ti_{0.34}Zr_{0.66})Mn_{0.86}V_{0.12}Cr_{0.11}Ni_{0.11}$ [43]	Dark	11.04	26.79	46.20	7.29	6.12	2.55	–
	Light	22.42	41.93	22.86	2.22	1.42	9.15	–
$(Ti_{0.34}Zr_{0.66})Mn_{0.84}V_{0.12}Cr_{0.12}Co_{0.12}$ [44]	Dark	9.71	26.76	45.25	6.26	7.95	–	4.08
	Light	17.54	41.09	28.93	3.66	3.25	–	5.53

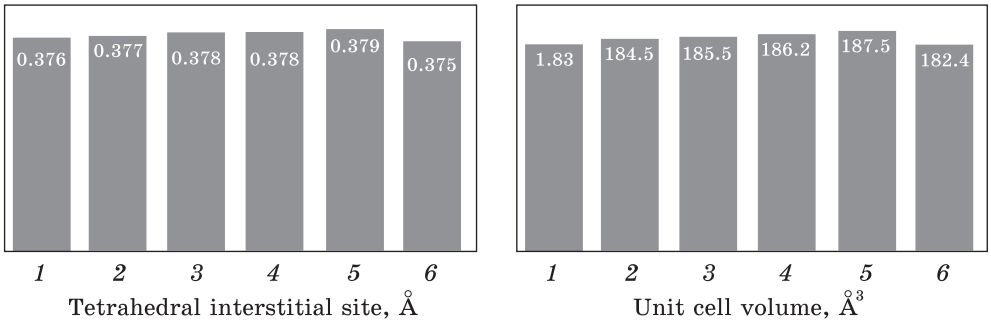

Fig. 3. Volume of unit cell and radius of tetrahedral interstitial site for *C*14-type Laves phase in different alloys: *1* — $(Ti_{0.34}Zr_{0.66})Mn_{1.2}$ [25]; *2* — $(Ti_{0.34}Zr_{0.66})Mn_{1.1}V_{0.1}$ [40]; *3* — $(Ti_{0.34}Zr_{0.66})Mn_{0.96}V_{0.12}Cr_{0.11}$ (titanium sponge) [39]; *4* — $(Ti_{0.34}Zr_{0.66})Mn_{0.86}V_{0.12}Cr_{0.11}Ni_{0.11}$ [43]; *5* — $(Ti_{0.34}Zr_{0.66})Mn_{0.96}V_{0.12}Cr_{0.11}$ (iodide titanium) [41]; *6* — $(Ti_{0.34}Zr_{0.66})Mn_{0.84}V_{0.12}Cr_{0.12}Co_{0.12}$ [44]

$R_s(C15) = 0.052662a$ with a being the lattice constant. The calculation was carried out only for interstitial sites of one type (A_2B_2). According to Refs. [51, 52], dissolved H atoms occupy only these interstitial sites in the *C*14-type Laves phase (Fig. 3).

As seen in Fig. 3, the partial substitution of manganese (atomic radius 0.127 nm) [54] with an element with a larger atomic radius (vanadium or chromium with atomic radius 0.134 and 0.130 nm, respectively) led to an increase in the unit cell volume. The radius of the tetrahedral interstitial site also increased, which is an effective way of affecting the amount of absorbed hydrogen, as was noted in [33].

The reduction in the unit cell volume and the radius of the tetrahedral interstitial site for the *C*14-type Laves phase in the $(Ti_{0.34}Zr_{0.66})Mn_{0.84}V_{0.12}Cr_{0.12}Co_{0.12}$ alloy was associated [44] with its chemical composition (Table 3). This phenomenon is the result of lower contents of titanium and zirconium (atomic radius 0.147 and 0.160 nm, respectively), which have significantly larger atomic radii compared to all other alloying elements [54]. Besides, the alloy additionally contains cobalt (atomic radius of 0.125 nm), which has a smaller atomic radius than other components. In addition, it is worthwhile to note that, according to the literature [55, 56], the partial substitution of manganese with cobalt should lead to a decrease in the above-mentioned parameters.

Based on the scanning electron microscopy (SEM) and x-ray phase analysis investigations, the authors of Refs. [39–42] concluded that when vanadium and chromium were added to the $(Ti_{0.34}Zr_{0.66})Mn_{1.2}$ alloy, the *C*14-type Laves phase preserved; however, the manganese content in this phase decreased to 44 at.%. This result is consistent with the data obtained in Ref. [57]. According to the phase diagram for the Ti–Mn binary system [58], the *C*14-type Laves phase is homogeneous at 59–70 at.% Mn. As we

showed earlier on an example of $(Ti_{0.34}Zr_{0.66})Mn_{1.2}$ alloy [25], the partial substitution of titanium with zirconium allows expanding this range to 54.4 at.% of Mn. In Refs. [59, 60], the mechanism of expansion of the Laves phase homogeneity field below 50 at.% Mn was explained. As shown on an example of the $Zr_{0.5}Ti_{0.5}Ni_{1.2}V_{0.5}Mn_{0.1}$ [57] (this composition corresponds to $AB_{1.8}$), the components of the system redistributed between positions *A* and *B* to form a stoichiometric AB_2 compound, as this compound is stable under equilibrium conditions. It was confirmed through the composition of the formed compound: $(Zr_{0.54}Ti_{0.46})(Ti_{0.04}Ni_{0.64}V_{0.27}Mn_{0.05})_2$. They explained this composition by the fact that when the component *B* lacks the exact AB_2 stoichiometry, some atoms of the component *A* (in this case Ti, since its atomic radius is close to that for Mn) move to unoccupied positions of the component *B* (Mn), so the stoichiometry AB_2 forms.

The above indicates that the addition of an element with a larger or smaller atomic radius (provided that the phase composition is preserved) leads to changes in the unit cell volume. This allows predicting the effect of a certain alloying element on the total hydrogen capacity of an alloy.

3. Hydrogen-Sorption Properties of the Alloys

The study of the interaction of the considered alloys with hydrogen under different conditions (isobaric–isothermal, isothermal, isobaric ones, and when temperature and pressure change simultaneously) was carried out in Refs. [39–44] using an IVGM-2M unit [61], which allowed experiments at 160–750 °C and hydrogen pressure 0.01–10 MPa.

To study the hydrogen-sorption properties of the materials, the samples were placed in a labyrinth-like crucible in the IVGM-2M unit chamber that was hermetically connected to the gas-vacuum system. When the pressure in the chamber reached 10^{-3}–10^{-4} Pa, thermosorption-purified hydrogen was let into it up to the target pressure. The labyrinth-like crucibles were used in order to minimize the mass losses of the sample during vacuuming, and the contamination of the hydrogenated sample. When the hydrogen pressure in the chamber was stabilized, visual and automatic recording of its changes was carried out. If necessary, the chamber was controllably heated to the temperature of the beginning of active hydrogen absorption or release, and then it was switched to isothermal mode. After isothermal exposure, the chamber was cooled to room temperature with the residual pressure. When the chamber was cooled down to room temperature, the hydrogen was pumped into one of the secondary chambers, where it was absorbed by a sorbent. The chamber was disconnected from the unit, opened, and the sample was removed for further analysis. The amount of absorbed or released hydrogen was determined by measuring pressures (volumetric method) before and after the experiment and was additionally controlled by weighing with an accuracy of $1.5 \cdot 10^{-5}$ grams

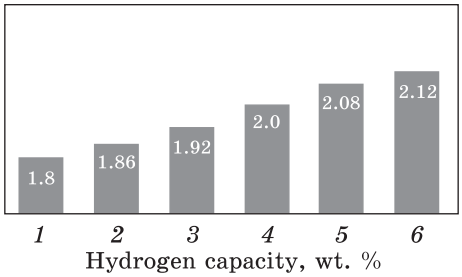

Fig. 4. Hydrogen capacity of different alloys: *1* — $(Ti_{0.34}Zr_{0.66})Mn_{1.2}$ [25]; *2* — $(Ti_{0.34}Zr_{0.66})Mn_{0.84}V_{0.12}Cr_{0.12}Co_{0.12}$ [44]; *3* — $(Ti_{0.34}Zr_{0.66})Mn_{0.86}V_{0.12}Cr_{0.11}Ni_{0.11}$ [43]; *4* — $(Ti_{0.34}Zr_{0.66})Mn_{1.1}V_{0.1}$ [40]; *5* — $(Ti_{0.34}Zr_{0.66})Mn_{0.96}V_{0.12}Cr_{0.11}$ (iodide titanium) [41]; *6* — $(Ti_{0.34}Zr_{0.66})Mn_{0.96}V_{0.12}Cr_{0.11}$ (titanium sponge) [42]

(gravimetric method). Several samples for each of the studied compositions (Table 1) were examined.

Since the alloys (Table 1, [25]) interacted with hydrogen at the same hydrogenation parameters (room temperature, hydrogen pressure in the range of 0.23–0.60 MPa, solid as-cast samples), a correct comparison of their hydrogen-sorption properties was possible.

The active absorption of hydrogen by all considered alloys (Table 1) at room temperature and hydrogen pressure in the range of 0.23–0.60 MPa began within 1–10 min (incubation period) after contact with a hydrogen-containing atmosphere. However, the process of interaction with hydrogen occurred in one or two stages, depending on the alloy composition. According to Refs. [39–42], the hydrogen absorption in the $(Ti_{0.34}Zr_{0.66})Mn_{1.2}$ [25], $(Ti_{0.34}Zr_{0.66})Mn_{1.1}V_{0.1}$, and $(Ti_{0.34}Zr_{0.66})Mn_{0.96}V_{0.12}Cr_{0.11}$ alloys occurred in one stage. These alloys absorbed almost all hydrogen in the first 15 min. The hydrogen capacities of the $(Ti_{0.34}Zr_{0.66})Mn_{1.1}V_{0.1}$ and $(Ti_{0.34}Zr_{0.66})Mn_{0.96}V_{0.12}Cr_{0.11}$ alloys were 2.00 and 2.12 wt.%, respectively (Fig. 4). Further exposure for 60 min did not lead to a significant change in the hydrogen capacity.

The hydrogen absorption in the $(Ti_{0.34}Zr_{0.66})Mn_{0.86}V_{0.12}Cr_{0.11}Ni_{0.11}$ [43] and $(Ti_{0.34}Zr_{0.66})Mn_{0.84}V_{0.12}Cr_{0.12}Co_{0.12}$ [44] alloys differed from the process described above and occurred in two stages. These alloys absorbed most of the dissolved H during the first 10 min of contact with a hydrogen-containing atmosphere (similarly to the parent alloy $(Ti_{0.34}Zr_{0.66})Mn_{1.2}$ [25]). The amount of absorbed H was 1.64 ± 0.03 wt.% for both alloys. Further exposure for 60 min with the same hydrogenation parameters led to an increase in the amount of absorbed H by 15 wt.%. The H capacity of $(Ti_{0.34}Zr_{0.66})Mn_{0.86}V_{0.12}Cr_{0.11}Ni_{0.11}$ and $(Ti_{0.34}Zr_{0.66})Mn_{0.84}V_{0.12}Cr_{0.12}Co_{0.12}$ alloys increased to 1.86 and 1.92 wt.%, respectively (Fig. 4). As shown in Refs. [43, 44], the hydrogen saturation of the *C*14-type Laves phase occurred at the first stage, *i.e.*, from the beginning of the hydrogen absorption to the hydrogen capacity of 1.64 ± 0.03 wt.% (this assumption was made based on the volume fractions of the phases and the amount of absorbed hydrogen). This led to the disintegration of the solid samples to the powder [62–64] and the formation of surfaces free of oxide scale [65]. At the second stage, the saturation of the second phase (based on the Zr_2Ni or

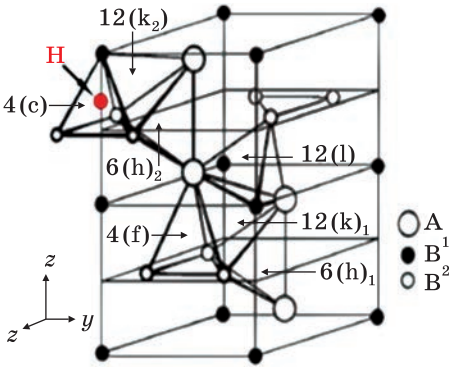

Fig. 5. Hexagonal crystal lattice of the *C*14-type Laves phase [66]

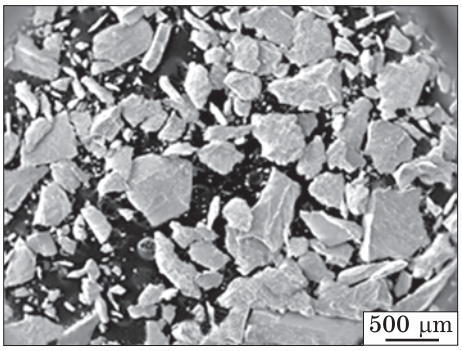

Fig. 6. Powder after hydrogenation [72]

Zr_2Co intermetallic compound, respectively) took place due to the already activated surface.

Further exposure of all the considered alloys under the same hydrogenation conditions for 24 h did not lead to an increase in their hydrogen capacity. Since the hydrogen absorption did not resume in 24 h, the authors [39–44] concluded that the alloys were saturated with hydrogen to the maximum possible level during this time.

A comparison of the hydrogen capacities of the considered alloys (Fig. 4) shows that the stable H capacity of the $(Ti_{0.34}Zr_{0.66})Mn_{1.2}$ [25] was increased by 15 wt.% due to the partial substitution of manganese (that does not interact with hydrogen) with elements which form stable chemical compounds with hydrogen.

The nature of increasing the hydrogen capacity when alloying with the above-mentioned elements becomes clear from the analysis made in Refs. [66, 67]. As shown in Ref. [67], there are three types of tetrahedral interstitial sites in the hexagonal AB_2 structure (Laves phase), which can be occupied by dissolved hydrogen (Fig. 5); the volume of these sites decreases in the sequence $A_2B_2 > AB_3 > B_4$. According to Ref. [66], hydrogen mainly occupies A_2B_2 interstitial sites in the alloys of this type, as they contain the maximum amount of *A* component (titanium, zirconium), which more actively interacts with hydrogen. Based on the above, the increase in the stable hydrogen capacity can be explained by the fact that some titanium atoms (as mentioned above) move to vacant positions of manganese atoms during the formation of the AB_2 compound. This leads to the redistribution of metal atoms that interact with hydrogen around the tetrahedral interstitial sites. In addition, the unit cell volume increases (except the $(Ti_{0.34}Zr_{0.66})Mn_{0.84}V_{0.12}Cr_{0.12}Co_{0.12}$ [44] alloy), so, the radius of the tetrahedral interstitial site also increases. Besides, the total amount of the component that forms a stable chemical compound with H in the *C*14-type Laves phase increased from 45.6 to 56 at.%.

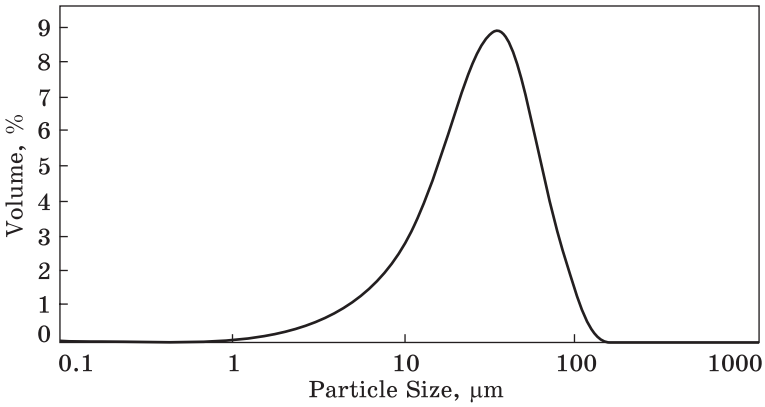

Fig. 7. Average size of powder

The solid samples were completely disintegrated to powder (Fig. 6) when all the above-mentioned alloys (Table 1) were saturated with hydrogen. This was caused by the high rate of the interaction process, as well as the low temperature of hydrogenation, and therefore, insufficient time for stress relaxation.

One can assume that the different amounts of hydrogen absorbed by the $(Ti_{0.34}Zr_{0.66})Mn_{0.96}V_{0.12}Cr_{0.11}$ alloy produced from titanium of different grades [39, 41] are related to the different content of impurities. The titanium sponge contained more impurities, which led to higher defect density in the final alloy. As known from the literature [68–71], the capture of hydrogen atoms by defects in the crystal lattice (vacancies, dislocations, *etc.*) plays a significant role during hydride formation. Most likely, the increase in the density of defects in crystal lattice led to a higher amount of absorbed hydrogen.

The hydrogenation of $(Ti_{0.34}Zr_{0.66})Mn_{0.84}V_{0.12}Cr_{0.12}Co_{0.12}$ alloy was studied in Ref. [44]. As shown in Fig. 7, a powder with an average particle size of 35 μm formed after the first hydrogenation, which coincides with other results [73]. Presumably, the formed powders had similar sizes because the process of hydrogen absorption occurred under similar conditions (room temperature and high absorption rate) for all considered alloys (Table 1).

According to the literature [73], all studied intermetallic compounds (AB_5, AB, and AB_2 types) turn into fine powders during the formation of hydrides and hydrogen-sorption–desorption cycles. This effect is called hydrogen decrepitation; it plays a very important role in the practical application of intermetallic compounds and hydrides based on them. According to [73], it causes negative consequences in some cases, *e.g.*, in hydrogen storage systems, and thermosorption compressors. In other cases, such as the development of materials for catalysis, hydrogen getters, magnets, and powder metallurgy, hydrogen decrepitation allows for improving the properties of materials [74, 75]. It was also shown in Ref. [73] that the reaction nature did not change, and only the reaction rate slightly increased

with the number of hydrogen-sorption–desorption cycles. The size of the powder after hydrogenation is determined by many parameters (number of cycles, pressure, and temperature). The major parameter is the number of sorption–desorption cycles. On an example of the AB_5 ($LaNi_5$) intermetallic compound, the author [73] showed that the average particle size was 50 μm after the first hydrogenation, 15 μm after 30 cycles, whereas it was 3.0 μm after 100 cycles.

X-ray phase analysis (Table 4) [39–44] did not show any changes in phase composition (formation of new phases or decomposition of initial ones) in the considered alloys (Table 1) after saturation with hydrogen. The results of Refs. [39–44] on the phase composition of the hydrogenation products coincide with the literature data [76]. According to Ref. [76], the crystal lattice of the metal matrix of the alloys based on the *C*14-type Laves phase persisted after their saturation with hydrogen. At the same time, the volume of unit cells increased isotropically by 20% (calculated by the difference in lattice constants before and after hydrogen saturation).

The H desorption from hydrogenation products of $(Ti_{0.34}Zr_{0.66})Mn_{1.2}$ [25], $(Ti_{0.34}Zr_{0.66})Mn_{1.1}V_{0.1}$ [40], and $(Ti_{0.34}Zr_{0.66})Mn_{0.96}V_{0.12}Cr_{0.11}$ [39, 41, 42] alloys was investigated using the automated dilatometric unit (ADU) with a mass spectrometer [77]. This unit was developed at the G.V. Kurdyumov Institute for Metal Physics of the National Academy of Sciences of Ukraine in order to the study the physical processes occurring in a process of the heating of powder compacts. The hydrogen release from the $(Ti_{0.34}Zr_{0.66})$

Table 4. **Lattice constants of phases after hydrogenation**

Alloys	Lattice constants ±0.0009 (nm)			
	λ-phase *C*14	λ-phase *C*15	Intermetallic compound Zr_2Ni	Intermetallic compound Zr_2Co
$(Ti_{0.34}Zr_{0.66})Mn_{1.2}$ [25]	$a = 0.5476$ $c = 0.8995$	—	—	—
$(Ti_{0.34}Zr_{0.66})Mn_{1.1}V_{0.1}$ [40]	$a = 0.5476$ $c = 0.8996$	—	—	—
$(Ti_{0.34}Zr_{0.66})Mn_{0.96}V_{0.12}Cr_{0.11}$ (titanium sponge) [39]	$a = 0.5490$ $c = 0.9018$	$a = 0.7665$	—	—
$(Ti_{0.34}Zr_{0.66})Mn_{0.96}V_{0.12}Cr_{0.11}$ (iodide titanium) [41]	$a = 0.5490$ $c = 0.9018$	$a = 0.7776$	—	—
$(Ti_{0.34}Zr_{0.66})Mn_{0.86}V_{0.12}Cr_{0.11}Ni_{0.11}$ [43]	$a = 0.5485$ $c = 0.9009$	—	$a = 1.2667$	—
$(Ti_{0.34}Zr_{0.66})Mn_{0.84}V_{0.12}Cr_{0.12}Co_{0.12}$ [44]	$a = 0.5469$ $c = 0.8917$	—	—	$a = 1.2455$

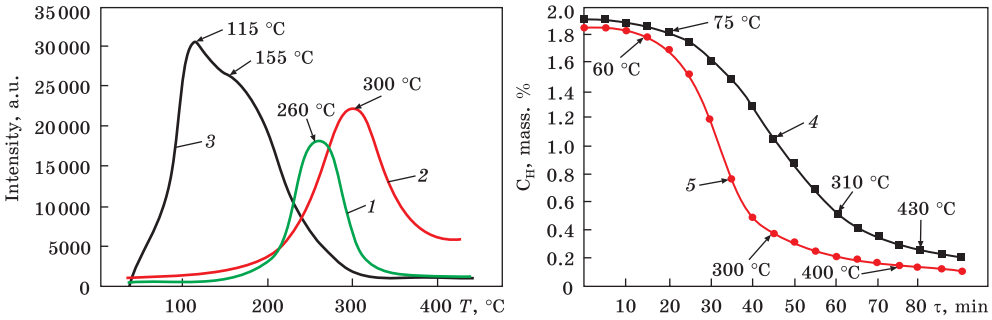

Fig. 8. Intensity of H release vs. temperature: $(Ti_{0.34}Zr_{0.66})Mn_{1.2}$ (*1*) [25]; $(Ti_{0.34}Zr_{0.66})Mn_{1.1}V_{0.1}$ (*2*) [40]; $(Ti_{0.34}Zr_{0.66})Mn_{0.96}V_{0.12}Cr_{0.11}$ (*3*) [39, 41, 42]; $(Ti_{0.34}Zr_{0.66})Mn_{0.86}V_{0.12}Cr_{0.11}Ni_{0.11}$ (*4*) [43]; $(Ti_{0.34}Zr_{0.66})Mn_{0.84}V_{0.12}Cr_{0.12}Co_{0.12}$ (*5*) [44]

$Mn_{0.86}V_{0.12}Cr_{0.11}Ni_{0.11}$ [43] and $(Ti_{0.34}Zr_{0.66})Mn_{0.84}V_{0.12}Cr_{0.12}Co_{0.12}$ [44] alloys was studied on IVGM-2M unit [61].

According to Refs. [25, 39–44], hydrogen begins to release from the hydrogenation products of all the alloys under consideration (Table 1) at an initial pressure of $4.0 \cdot 10^{-3}$ Pa at room temperature, regardless of the grade of titanium used. These desorption parameters allowed removing no more than 4.0% of the total amount of absorbed hydrogen. Further hydrogen release from the mixture of hydrides occurred under heating (Fig. 8).

The partial substitution of manganese in the $(Ti_{0.34}Zr_{0.66})Mn_{1.2}$ alloy by vanadium and chromium led to a significant decrease in the thermal stability of the hydride (see Fig. 8). In all other cases, alloying led to higher hydride stability.

The temperature of the maximum intensity of hydrogen release in the $(Ti_{0.34}Zr_{0.66})Mn_{1.1}V_{0.1}$, $(Ti_{0.34}Zr_{0.66})Mn_{0.86}V_{0.12}Cr_{0.11}Ni_{0.11}$, and $(Ti_{0.34}Zr_{0.66})Mn_{0.84}V_{0.12}Cr_{0.12}Co_{0.12}$ alloys increased by 40 ± 10 °C as compared to the $(Ti_{0.34}Zr_{0.66})Mn_{1.2}$ alloy (Fig. 8). Accordingly, the temperature of complete desorption of hydrogen also increased. In Ref. [40], the whole of absorbed H was released from the $(Ti_{0.34}Zr_{0.66})Mn_{1.1}V_{0.1}$ alloy at 400 °C (and at 350 °C from the $(Ti_{0.34}Zr_{0.66})Mn_{1.2}$ alloy [25]). At the same time, only 90 ± 5.0% of the total amount of absorbed hydrogen was released after heating up to 430 °C in Refs. [43, 44].

The increase in thermal stability of the final hydride in Refs. [40, 43, 44] was explained basing on the literature data. A similar increase in the thermal stability of the hydride formed after the saturation of the $(Ti_{0.9}Zr_{0.1})Mn_{1.2}V_{0.1}$ alloy with hydrogen was observed in Ref. [37]. The authors [37] associated the increase in the thermal stability of the hydride by the fact that the component *A* (titanium with its high affinity for hydrogen and a high desorption temperature above 350 °C [78, 79]) partially moved to the unoccupied sites of the component *B* (manganese). In addition, the partial substitution of manganese as the component *B* with

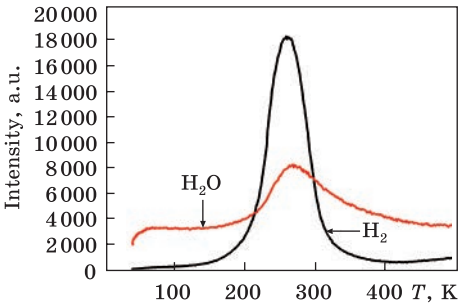

Fig. 9. Dependence of intensity of hydrogen and water vapour release on the temperature for $(Ti_{0.34}Zr_{0.66})Mn_{1.2}$ alloy [25]

other elements leads to the transformation of a part of the tetrahedral interstitial sites from the A_2B_2 to A_3B ones, which is more favourable for hydrogen accumulation, as well as the transformation from AB_3 in A_2B_2 sites. Besides, the increase in the thermal stability of the hydride is also affected by the presence of the second phase [43, 44].

The process of hydrogen release in the $(Ti_{0.34}Zr_{0.66})Mn_{0.96}V_{0.12}Cr_{0.11}$ alloy significantly differs from the other considered alloys, regardless of the titanium grade used (Fig. 8) [39, 41, 42]. As seen in Fig. 8, the hydrogen release actively occurred at the beginning of heating; the maximum rate was registered at 115±10 °C (for other alloys 300±10 °C), and at 300±10 °C all hydrogen was released. The presented curves (Fig. 8.) The $(Ti_{0.34}Zr_{0.66})Mn_{0.96}V_{0.12}Cr_{0.11}$ alloy did not have a long stage with a low rate of hydrogen release, which was observed for other alloys (see Fig. 8). Another feature of the hydrogen release from the $(Ti_{0.34}Zr_{0.66})Mn_{0.96}V_{0.12}Cr_{0.11}$ alloy is the splitting of the peak (Fig. 8). This splitting was related to the release of hydrogen from the hydrides based on two Laves phases of the *C*14 and *C*15 types, which have different thermal stabilities [39, 41, 42].

According to the literature [80, 81], the thermal stability of the hydrides based on the AB_2 intermetallic compounds (Laves phase) can be reduced (without a significant loss in hydrogen capacity and hydrogen absorption kinetics) by the partial substitution of *A* or *B* atoms by other elements. In addition, electronic or chemical effects [82, 83] can cause a decrease in thermal stability. Based on the literature [51, 84], the authors of Refs. [39, 41, 42] supposed that the hydride based on the *C*15-type Laves phase had lower thermal stability as compared to that based on the *C*14-type phase. This explains the significant difference in the hydrogen desorption between the $(Ti_{0.34}Zr_{0.66})Mn_{0.96}V_{0.12}Cr_{0.11}$ alloy (which contains the *C*14- and *C*15-type Laves phases) and all other considered alloys (Table 1).

As shown [25, 39–42], the traces of water vapour appeared when the temperature of maximum hydrogen release was reached (Fig. 9). This indicates that released atomic hydrogen reduces the oxide scale [85, 86], which is always present on the surface of titanium Ti-based alloys. In this way, the surface is refined. Firstly, it accelerates the kinetics of hydrogen sorption–desorption, since the oxide scale is a barrier to hydrogen diffusion. Secondly, the probability of rapid degradation of the hydrogen-sorption properties of an alloy significantly decreases with the number of cycles. This allows increasing the number of sorption–desorption cycles,

which is important for practical use, without significant losses in hydrogen capacity [87].

The preservation of hydrogen-sorption properties after multiple hydrogen-sorption–desorption cycles is an important parameter for the alloys designed for hydrogen storage. Taking into account this fact, the authors of [39–44] studied the considered alloys (Table 1). The second cycle of hydrogen sorption was realized at room temperature at a total pressure of 0.21 MPa, which was somewhat lower than for the first hydrogenation. The hydrogenation pressure was reduced to prove the enhancement of hydrogen-sorption characteristics after the first sorption–desorption cycle, which activated the material [23]. According to the authors, the saturation of these alloys with hydrogen at a low pressure makes the process safer, and the hydrogen battery lighter, which is especially important for practical use in transport.

After the first sorption–desorption cycle, the hydrogen absorption by all considered alloys (Table 1) began from the first seconds of contact of the sample with a hydrogen-rich atmosphere at a high rate, while the hydrogen capacity remained unchanged [39–44]. This enhancement in the hydrogen-sorption properties of the alloys during the second cycle (reduction of hydrogenation pressure to 0.21 MPa, as well as reduction of the incubation period from several min to several seconds) was explained by the activated state of the material after the first sorption–desorption cycle. Firstly, the solid samples were defragmented to a powder, which led to an increase in the specific surface (including the formation of new juvenile surfaces) [88, 89]. Secondly, the barrier oxide scale on the previously existing surfaces was partially restored as a result of their interaction with atomic hydrogen, which was released during the first desorption cycle [90].

4. Conclusions

• Partial substitution of manganese (which does not form hydrides) with elements that interact with hydrogen in the Ti–Zr–Mn system alloy with the *C*14-type Laves phase led to an increase in the hydrogen capacity.

• When the alloys based on the *C*14-type Laves phase are saturated with hydrogen, their phase composition does not change, regardless of their initial phase composition and the method of alloy production. The initial phases transform into hydrides based on them.

• Regardless of the initial phase and chemical composition of the alloys of the considered systems, their preliminary activation by the hydrogen-sorption–desorption cycle is useful. This activation does not reduce the hydrogen capacity during subsequent sorption–desorption cycles and significantly accelerates the kinetics of hydrogenation, reducing the time required to reach the maximum possible concentration of hydrogen in the alloy.

• Complete substitution of a high-cost component of the alloy (iodide titanium) with a cheaper one (TG-110 grade titanium sponge) allowed reducing the cost of the hydride without losing hydrogen absorption properties, and thereby, increasing the competitiveness of the materials of this type.

Acknowledgement. This work was carried out within the framework of the personal grant of the Verkhovna Rada (Parliament) of Ukraine for young scientists–doctors of sciences for 2023 (State Reg. No. 0123U103625).

REFERENCES

1. D. Shaltiel, I. Jacob, and D. Davidov, Hydrogen Absorption and Desorption Properties of AB_2 Laves-phase Pseudobinary Compounds, *J. Less-Common Met.*, **53**: 117–131 (1977); https://doi.org/10.1016/0022-5088(77)90162-X
2. I. Jacob, D. Shaltiel, D. Davidov, and I. Miloslavski, A Phenomenological Model for the Hydrogen Absorption Capacity in Pseudobinary Laves Phase Compounds, *Solid State Commun.*, **23**: 669–672 (1977); https://doi.org/10.1016/0038-1098(77)90546-4
3. I. Jacob and D. Shaltiel, Hydrogen Absorption in $Zr(Al_xFe_{1-x})_2$ Laves Phase Compounds, *Solid State Commun.*, **27**: 175–180 (1978); https://doi.org/10.1016/0038-1098(78)90826-8
4. H. Oesterreicher and H. Bittner, Studies of Hydride Formation in $Ti_{1-x}Zr_xMn_2$, *Mat. Res. Bull.*, **13**: 83–88 (1978); https://doi.org/10.1016/0025-5408(78)90031-4
5. D.P. Shoemaker and C.B. Shoemaker, Concerning Atomic Sites and Capacities for Hydrogen Absorption in the AB_2 Friauf–Laves Phases, *J. Less-Common Met.*, **68**: 43–58 (1979); https://doi.org/10.1016/0022-5088(79)90271-6
6. X. Li, D. Wu, Q. Zhou, R. Tang, Y. Zhu, F. Xiao, W. Li, and H.-J. Lin, Improved Hydrogen Storage Properties of Low-cost Ti–Cr–V Alloys by Minor Alloying of Mn, *Int. J. Hydrogen Energy*, **50**: 224–234 (2024); https://doi.org/10.1016/j.ijhydene.2023.07.020
7. M. Piao, X. Xiao, L. Zhan, Z. Cao, P. Zhou, J. Qi, M. Lu, Z. Li, L. Jiang, F. Fang, and L. Chen, Laves Phase Double Substitution Alloy Design and Device Filling Modification for Ti-Based Metal Hydride Hydrogen Compressors, *Int. J. Hydrogen Energy*, **50**: 1358–1368 (2024); https://doi.org/10.1016/j.ijhydene.2023.09.228
8. X. Zhang, B. Li, L. Wang, W. Xiong, J. Li, S. Zhou, J. Xu, Y. Zhao, X. He, and H. Yan, Hydrogen Storage Properties of AB_2 Type Ti–Zr–Cr–Mn–Fe Based Alloys, *Int. J. Hydrogen Energy*, **51**: 193–201 (2024); https://doi.org/10.1016/j.ijhydene.2023.11.045
9. L. Yang, Y. Zhiyi, Z. Panpan, X. Xuezhang, Q. Jiacheng, B. Jiapeng, H. Xu, K. Huaqin, and C. Lixin, A Review of Classical Hydrogen Isotopes Storage Materials, *Mater. Rep. Energy*, **4**: 100250 (2024); https://doi.org/10.1016/j.matre.2024.100250
10. V.A. Dekhtyarenko, Composite Material Based on Laves Phase with Magnesium for Hydrogen Storage, *MRS Communications*, **14**: 337–344 (2024); https://doi.org/10.1557/s43579-024-00534-7

11. M. Lototskyy, I. Tolj, Y. Klochko, M.W. Davids, D. Swanepoel, and V. Linkov, Metal Hydride Hydrogen Storage Tank for Fuel Cell Utility Vehicles, *Int. J. Hydrogen Energy,* **45**: 7958–7967 (2020); https://doi.org/10.1016/j.ijhydene.2019.04.124
12. V.A. Yartys and M.V. Lototskyy, Laves Type Intermetallic Compounds as Hydrogen Storage Materials: A Review, *J. Alloys Compd.*, **916**: 165219 (2022); https://doi.org/10.1016/j.jallcom.2022.165219
13. P. Ma, W. Li, and E. Wu, Hydrogen Activation and Storage Properties of Laves Phase $Ti_{1-x}Sc_xMn_{1.6}V_{0.4}$ Alloys, *Int. J. Hydrogen Energy*, **46**: 34389–34398 (2021); https://doi.org/10.1016/j.ijhydene.2021.08.017
14. W. Qiao, D. Yin, S. Zhao, N. Ding, L. Liang, C. Wang, L. Wang, M. He, and Y. Cheng, Effects of Cu Doping on the Hydrogen Storage Performance of Ti-Mn-based, AB_2-Type Alloys, *Chem. Eng. J.*, **465**: 142837 (2023); https://doi.org/10.1016/j.cej.2023.142837
15. J.L. Bobet, B. Chevalier, and T.B. Darrie, Crystallographic and Hydrogen Sorption Properties of $TiMn_2$ Based Alloys, *Intermettallics*, **8**, No. 4: 359–363 (2000); https://doi.org/10.1016/S0966-9795(99)00092-8
16. X. Yu, B. Xia, Z. Wu, and N. Xu, Phase Structure and Hydrogen Sorption Performance of Ti–Mn-Based Alloys, *Mat. Sci. Eng. A*, **373**, Nos. 1–2: 303–308 (2004); https://doi.org/10.1016/j.msea.2004.02.008
17. S. Samboshi, N. Masahashi, and S. Hanada, Effect of Composition on Hydrogen Absorbing Properties in Binary $TiMn_2$ Based Alloys, *J. Alloys Compd.*, **352**: 210–217 (2003); https://doi.org/10.1016/S0925-8388(02)01125-8
18. V. Ivanchenko, V. Dekhtyarenko, T. Kosorukova, and T. Pryadko, Phase Equilibria in the $TiMn_2$–$TiFe_2$, Polythermal Section, *Chem. Met. Alloys*, **1**, No. 2: 137–139 (2008); https://doi.org/10.30970/cma1.0045
19. W. Jian, C. He, X. Yang, X. Xiao, L. Ouyang, and M. Zhu, Influence of Element Substitution on Structural Stability and Hydrogen Storage Performance: A Theoretical and Experimental Study on $TiCr_{2-x}Mn_x$ Alloy, *Renewable Energy*, **197**: 564–573 (2022); https://doi.org/10.1016/j.renene.2022.07.113
20. P. Zhou, Z. Cao, X. Xiao, L. Zhan, J. He, Y. Zhao, Li Wang, Mi Yan, Z. Li, and L. Chen, Development of RE-Based and Ti-Based Multicomponent Metal Hydrides with Comprehensive Properties Comparison for Fuel Cell Hydrogen Feeding System, *Mater. Today Energy*, **33**: 101258 (2023); https://doi.org/10.1016/j.mtener.2023.101258
21. Yh. Zhang, C. Li, W. Zhang, X. Wei, J. Li, Y. Qi, and Dong-liang Zhao, Research and Application of Ti–Mn-Based Hydrogen Storage Alloys, *J. Iron Steel Res. Int.*, **30**: 611–625 (2023); https://doi.org/10.1007/s42243-022-00905-1
22. J.L. Bobet and T.B. Darriet, Relationship Between Hydrogen Sorption Properties and Crystallography for $TiMn_2$ Based Alloys, *Int. J. Hydrogen Energy*, **25**: 767–772 (2000); https://doi.org/10.1016/S0360-3199(99)00101-9
23. X.Y. Song, Y. Chen, Z. Zhang, Y.Q. Lei, X.B. Zhang, and Q.D. Wang, Microstructure and Electrochemical Properties of Ti-containing AB_2 Type Hydrogen Storage Electrode Alloy, *Int. J. Hydrogen Energy*, **25**: 649–656 (2000); https://doi.org/10.1016/S0360-3199(99)00080-4

24. J.G. Park, H.Y. Jang, S.C. Han, P.S. Lee, and J.Y. Lee, Hydrogen Storage Properties of $TiMn_2$-Based Alloys for Metal Hydride Heat Pump, *Mat. Sci. Eng. A*, **329–331**: 351–355 (2002); https://doi.org/10.1016/S0921-5093(01)01598-2
25. V.G. Ivanchenko, V.A. Dekhtyarenko, and T.V. Pryadko, Hydrogen-Sorption Properties of (Ti, Zr)Mn_{2-x} Intermetallic Alloy, *Powder Metall. Met. Ceram.*, **52**: 340–344 (2013); https://doi.org/10.1007/s11106-013-9531-9
26. G. Andrade, B. H. Silva, G. Zepon, and R. Floriano, Hydrogen Storage Properties of Zr-Based Multicomponent Alloys with *C*14-Laves Phase Structure Derived from the Zr–Cr–Mn–Fe–Ni System, *Int. J. Hydrogen Energy*, **51**: 246–254 (2024); https://doi.org/10.1016/j.ijhydene.2023.11.111
27. V.A. Dekhtyarenko, D.G. Savvakin, V.I. Bondarchuk, V.M. Shyvanyuk, T.V. Pryadko, and O.O. Stasiuk, $TiMn_2$-Based Intermetallic Alloys for Hydrogen Accumulation: Problems and Prospects, *Prog. Phys. Met.*, **22**, No. 3: 307–351 (2021); https://doi.org/10.15407/ufm.22.03.307
28. H. Zhao, P. Yao, Y. Zhao, Z. Zeng, C. Xia, and T. Yang, Microstructure and Hydrogen Storage Properties of Zr-Based AB_2-Type High Entropy Alloys, *J. Alloys Compd.*, **960**: 170665 (2023); https://doi.org/10.1016/j.jallcom.2023.170665
29. H. Smithson, C.A. Marianetti, D. Morgan, A. Van der Ven, A. Predith, and G. Ceder, First-Principles Study of the Stability and Electronic Structure of Metal Hydrides, *Phys. Rev. B*, **66**, No. 12: 144107 (2002); https://doi.org/10.1103/PhysRevB.66.144107
30. K. Young, D. F. Wong, and L. Wang, Effect of Ti/Cr Content on the Microstructures and Hydrogen Storage Properties of Laves Phase-Related Body-Centered-Cubic Solid Solution Alloys, *J. Alloys Compd.*, **622**: 885–893 (2015); https://doi.org/10.1016/j.jallcom.2014.11.006
31. R.R. Jeng, C.Y. Chou, S.-L. Lee, Y.C. Wu, and H.Y. Bor, Effect of Mn, Ti/Cr Rratio, and Heat Treatment on Hydrogen Storage Properties of Ti–V–Cr–Mn Alloys, *J. Chin. Inst. Eng.*, **34**, No. 5: 601–608 (2011); https://doi.org/10.1080/02533839.2011.577595
32. D.N. Movchan, V.N. Shyvanyuk, B.D. Shanina, and V.G. Gavriljuk, Atomic Interactions and Hydrogen-Induced γ Phase in FCC Iron–Nickel Alloys, *Phys. Status Solidi A*, **207**: 1796–1801 (2010); https://doi.org/10.1002/pssa.200925548
33. P. Liu, X. Xie, L. Xu, X. Li, and T. Liu, Hydrogen Storage Properties of $(Ti_{0.85}Zr_{0.15})_{1.05}Mn_{1.2}Cr_{0.6}V_{0.1}M_{0.1}$ (M = Ni, Fe, Cu) Alloys Easily Activated at Room Temperature, *Prog. Nat. Sci.*, **27**: 652–657 (2017); https://doi.org/10.1016/j.pnsc.2017.09.007
34. M. Hara, K. Yudou, E. Kinoshita, K. Okazaki, K. Ichinose, K. Watanabe, and M. Matsuyama, Alloying Effects on the Hydride Formation of $Zr(Mn_{1-x}Co_x)_2$, *Int. J. Hydrogen Energy*, **36**: 12333–12337 (2011); https://doi.org/10.1016/j.ijhydene.2011.07.024
35. S.V. Mitrokhin, T.N. Bezuglaya, and V.N. Verbetsky, Structure and Hydrogen Sorption Properties of (Ti,Zr)–Mn–V Alloys *J. Alloys Compd.*, **330–332**: 146–151 (2002); https://doi.org/10.1016/S0925-8388(01)01469-4
36. X.B. Yu, J.Z. Chen, Z. Wu, B.J. Xia, and N.X. Xu, Effect of Cr Content on Hydrogen Storage Properties for Ti–V–Based BCC-Phase Alloys, *Int. J. Hydrogen Energy*, **29**: 1377–1381 (2004); https://doi.org/10.1016/j.ijhydene.2004.01.015

37. E.A. Anikina and V.N. Verbetsky, Calorimetric Investigation of the Hydrogen Interaction with $Ti_{0.9}Zr_{0.1}Mn_{1.2}V_{0.1}$, *Int. J. Hydrogen Energy*, **36**: 1344–1348 (2011); https://doi.org/10.1016/j.ijhydene.2010.06.085
38. T.V. Pryadko, Features of Hydrogenation of the T–V System Alloys, *Metallofiz. Noveishie Tekhnol.*, **37**, No. 2: 243–255 (2015) (in Russian); https://doi.org/10.15407/mfint.37.02.0243
39. V.A. Dekhtyarenko, Alloy Based on Intermetallic (Ti, Zr)(V, Mn, Cr)$_{2-x}$ Obtained Using Titanium Sponge for Hydrogen Sorption, *Metallofiz. Noveishie Tekhnol.*, **41**, No. 10: 1283–1290 (2019); https://doi.org/10.15407/mfint.41.10.1283.
40. V.A. Dekhtyarenko, Structure and Hydrogen Sorption Properties of $(Ti_{0.34}Zr_{0.66})Mn_{1.11}V_{0.1}$ Alloy, *Metallofiz. Noveishie Tekhnol.*, **37**, No. 5: 683–688 (2015) (in Russian); https://doi.org/10.15407/mfint.37.05.0683
41. T.V. Pryadko and V.A. Dekhtyarenko, Influence of Partial Substitution of Manganese with Chromium on Structure and Kinetics of Hydrogenation of an Alloy Based on the (Ti, Zr)(V, Mn)$_{2-x}$ Intermetallide, *Metallofiz. Noveishie Tekhnol.*, **40**, No. 5: 649–660 (2018) (in Russian); https://doi.org/10.15407/mfint.40.05.0649
42. V.A. Dekhtyarenko, Hydrogen Storage Properties of $Ti_{15.4}Zr_{30.2}Mn_{44}V_{5.4}Cr_5$ Alloy Produced by Induction and Arc Melting, *Metallofiz. Noveishie Tekhnol.*, **43**, No. 8: 1053–1063 (2021); https://doi.org/10.15407/mfint.43.08.1053
43. H.Y. Mykhailova, V.A. Dekhtyarenko, and Y.V. Vasylyk, Hydrogen Sorption Properties of $Ti_{15.4}Zr_{30.2}Mn(_{54.4-x-y})V_xCr_yNi_y$ Alloy Able of Being Activated at Room Temperature and Pressure of 0.23 MPa, *MRS Communications*, **13**: 1288–1295 (2023); https://doi.org/10.1557/s43579-023-00451-1
44. V.A. Dekhtyarenko, Hydrogen-Sorption Properties of the Alloy $Ti_{15.5}Zr_{30}Mn_{38}V_{5.5}Cr_{5.5}Co_{5.5}$ Based on the Laves Phase (Type *C*14), *Metallofiz. Noveishie Tekhnol.*, **45**, No. 6: 743–755 (2023); https://doi.org/10.15407/mfint.45.06.0743
45. H. Kazemipour, A. Salimijazi, A. Saidi, A. Saatchi, and A. Arefarjmand, Hydrogen Storage Properties of $Ti_{0.72}Zr_{0.28}Mn_{1.6}V_{0.4}$ Alloy Prepared by Mechanical Alloying and Copper Boat Induction Melting, *Int. J. Hydrogen Energy*, **39**: 12784–12788 (2014); https://doi.org/10.1016/j.ijhydene.2014.06.085
46. Y. Zhang, J. Li, T. Zhang, T. Wu, H. Kou, and X. Xue, Hydrogenation Thermokinetics and Activation Behavior of Non-Stoichiometric Zr-Based Laves Alloys with Enhanced Hydrogen Storage Capacity, *J. Alloys Compd.*, **694**: 300–308 (2017); https://doi.org/10.1016/j.jallcom.2016.10.021
47. S. Suwarno, J.K. Solberg, V.A. Yartys, and B. Krogh, Hydrogenation and Microstructural Study of Melt-Spun $Ti_{0.8}V_{0.2}$, *J. Alloys Compd.*, **509**: S775–S778 (2011); https://doi.org/10.1016/j.jallcom.2010.10.130
48. P. Pei, X.P. Song, J. Liu, M. Zhao, and G.L. Chen, Improving Hydrogen Storage Properties of Laves Phase Related BCC Solid Solution Alloy by SPS Preparation Method, *Int. J. Hydrogen Energy*, **34**: 8597–8602 (2009); https://doi.org/10.1016/j.ijhydene.2009.08.038
49. B. Predel, *Cr–Zr (Chromium-Zirconium)* (Berlin–Heidelberg: Springer-Verlag: 1994).
50. J.R. Johnson, Reaction of Hydrogen with the High Temperature (*C*14) form of $TiCr_2$, *J. Less-Common Met.*, **73**: 345–354 (1980); https://doi.org/10.1016/0022-5088(80)90328-8

51. J. Bodega, J.F. Fernández, F. Leardini, J.R. Ares, and C. Sánchez, Synthesis of Hexagonal *C*14/C36 and Cubic *C*15 $ZrCr_2$ Laves Phases and Thermodynamic Stability of Their Hydrides, *J. Phys. Chem. Solids*, **72**, No. 11: 1334–1342 (2011); https://doi.org/10.1016/j.jpcs.2011.08.004
52. T.L. Murashkina, *Patterns of Change in the Structural-Phase State and Defective Structure of the Laves Intermetallic Phase of the C36 $TiCr_2$ Structural Polytype during Cyclic Hydrogen Sorption/Desorption Processes* (Abstract of Diss. Candidate of Physical and Mathematical Sciences) (Tomsk: National Research Tomsk Polytechnic University: 2018) (in Russian).
53. V.A. Dekhtyarenko, T.V. Pryadko, D.G. Savvakin, and V.I. Bondarchuk, Structure, Phase Composition, and Hydrogen Absorption Properties of Multiphase Alloys of Ti–Zr–Mn–V System Alloyed with Holmium, *Metallofiz. Noveishie Tekhnol.*, **44**, No. 7: 913–926 (2022); https://doi.org/10.15407/mfint.44.07.0913
54. N.N. Greenwood and A. Earnshaw, *Chemistry of the Elements* (Oxford: Butterworth Heinemann: 1997).
55. S. Hong and C.L. Fu, Hydrogen in Laves Phase ZrX_2 (X = V, Cr, Mn, Fe, Co, Ni) Compounds: Binding Energies and Electronic and Magnetic Structure, *Phys. Rev. B*, **66**: 094109 (2002); https://doi.org/10.1103/PhysRevB.66.094109
56. C. Weng, X. Xiao, X. Huang, F. Jiang, Z. Yao, S. Li, H. Ge, and, L. Chen, Effect of Mn Substitution for Co on the Structural, Kinetic, and Thermodynamic Characteristics of $ZrCo_{1-x}Mn_x$ (x = 0–0.1) Alloys for Tritium Storage, *Int. J. Hydrogen Energy*, **42**: 28498–28506 (2017); https://doi.org/10.1016/j.ijhydene.2017.09.157
57. S.V. Mitrokhin, Regularities of Hydrogen Interaction with Multicomponent Ti(Zr)–Mn–V Laves Phase Alloys, *J. Alloys Compd.*, **404–406**: 384–387 (2005); https://doi.org/10.1016/j.jallcom.2005.02.078
58. V.G. Ivanchenko, I.S. Gavrylenko, V.V. Pogorelaya, V.I. Nychyporenko, and T.V. Pryadko, Study of Phase Equilibria in Alloys of the System Ti–Mn, *Metaloznav. Obrob. Met.*, **4**: 16–20 (2004) (in Ukrainian).
59. T.A. Zotov, V.N. Verbetskii, T.Ya. Safonova, A.V. Garshev, and O.A. Petriiz, Hydrogen Sorption and Electrochemical Properties of Alloys: Systems Zr–Ti–Ni–V–Mn with Laves Phase Structures, *Russ. J. Electrochem.*, **43**, No. 3: 355–363 (2007); https://doi.org/10.1134/S1023193507030147
60. F. Stein and A. Leineweber, Laves Phases: a Review of Their Functional and Structural Applications and an Improved Fundamental Understanding of Stability and Properties, *J. Mater. Sci.*, **56**: 5321–5427 (2021); https://doi.org/10.1007/s10853-020-05509-2
61. G.F. Kobzenko and A.A. Shkola, Reactor for Studying Physical and Chemical Processes of Gas Saturation, *Zavodskaya Laboratoriya*, **7**: 41–45 (1990) (in Russian).
62. V.G. Ivanchenko, V.A. Dekhtyarenko, and T.V. Pryadko, Sorption Properties of Heterophase Alloys b(Ti, Zr, Mn) + (Ti, Zr)Mn_{2-x}, *Metallofiz. Noveishie Tekhnol.*, **33**, Spec. Iss.: 479–484 (2011) (in Russian).
63. V.G. Ivanchenko, V.A. Dekhtyarenko, T.V. Pryadko, D.G. Savvakin, and I.K. Evlash, Influence of Heat Treatment on the Hydrogen-Sorption Properties of $Ti_{0.475}Zr_{0.3}Mn_{0.225}$ Eutectic Alloy Doped with Vanadium, *Mater. Sci.*, **51**, 492–499 (2016); https://doi.org/10.1007/s11003-016-9867-7
64. V.A. Dekhtyarenko, T.V. Pryadko, D.G. Savvakin, V.I. Bondarchuk, and G.S. Mogylnyy, Hydrogenation Process in Multiphase Alloys of Ti–Zr–Mn–V System on

the Example of $Ti_{42.75}Zr_{27}Mn_{20.25}V_{10}$ Alloy, *Int. J. Hydrogen Energy*, **46**: 8040–8047 (2021);
https://doi.org/10.1016/j.ijhydene.2020.11.283

65. V.G. Ivanchenko, V.A. Dekhtyarenko, and T.V. Pryadko, Hydrogen Sorption Properties of $Ti_{0.475}Zr_{0.3}Mn_{0.225}$ Eutectic Alloy Alloyed with 2 at.% and 5 at.% of Vanadium, *Metallofiz. Noveishie Tekhnol.*, **37**, No. 4: 521–530 (2015);
https://doi.org/10.15407/mfint.37.04.0521
66. V.A. Dekhtyarenko, *Regularities and Mechanisms of Interaction of Hydrogen with Multicomponent Titanium Alloys Based on Laves Phases and B.C.C. Solid Solution* (Abstract of Thesis for Dr. Tech. Sci.) (Kyiv: G.V. Kurdyumov Institute for Metal Physics, N.A.S.U.: 2021) (in Ukrainian).
67. H. Kohlmann, Hydrogen Order in Hydrides of Laves Phases, *Z. Kristallogr. Cryst. Mater.*, **235**: 319–332 (2020);
https://doi.org/10.1515/zkri-2020-0043
68. Y. Tateyama and T. Ohno, Stability and Clusterization of Hydrogen–Vacancy Complexes in α-Fe: An ab Initio Study, *Phys. Rev. B*, **67**: 174105 (2003);
https://doi.org/10.1103/PhysRevB.67.174105
69. Y. Fukai, The Metal–Hydrogen System (Berlin: Springer: 2005)
https://doi.org/10.1007/3-540-28883-X
70. M. Tamura and T. Eguchi, Nanostructured Thin Films for Hydrogen-Permeation Barrier, *J. Vac. Sci. Technol. A*, **33**: 0415031–0415036 (2015);
https://doi.org/10.1116/1.4919736
71. J.G. Niu and W.T. Geng, Oxygen-Induced Lattice Distortion in β-Ti_3Nb and its Suppression Effect on β to α″ Transformation, *Acta Mater.*, **81**: 194–203 (2014);
https://doi.org/10.1016/j.actamat.2014.07.060
72. V. Dekhtyarenko, Structure, Phase Composition and Hydrogen Sorption Properties of Eutectic Alloy $Ti_{47.5}Zr_{30.2}Mn_{22.5}$ Obtained Using Titanium Sponge, *Mater. Sci. Non-Equilibrium Phase Transformations,* **5**, No. 3: 78–80 (2019).
73. V.N. Verbetsky, *Synthesis and Properties of Multicomponent Metal Hydrides* (Abstract of Diss. Doctor of Chemical Sciences) (Moskva: Lomonosov Moscow State University: 1998) (in Russian).
74. O.M. Ivasyshyn and D.H. Savvakin, Synthesis of Zirconium and Titanium-Based Alloys with the Use of Their Hydrides, *Mater. Sci.*, **51**: 465–474 (2016);
https://doi.org/10.1007/s11003-016-9863-y
75. O.M. Ivasyshyn, D.H. Savvakin, V.A. Dekhtyarenko, and O.O. Stasyuk, Interaction of Ti–Al–V–Fe, Al–V–Fe, and Ti–Al–Mo–Fe Powder Master Alloys with Hydrogen, *Mater. Sci.*, **54**: 266–272 (2018);
https://doi.org/10.1007/s11003-018-0182-3
76. S.V. Mitrokhin, T.N. Smirnova, V.A. Somenkov, V.P. Glazkov, and V.N. Verbetsky, Structure of (Ti,Zr)–Mn–V Nonstoichiometric Laves Phases and $(Ti_{0.9}Zr_{0.1})(Mn_{0.75}V_{0.15}Ti_{0.1})_2D_{2.8}$ Deuteride, *J. Alloys Compd.*, **356–357**: 80–83 (2003);
https://doi.org/10.1016/S0925-8388(03)00257-3
77. O.M. Ivasishin, V.T. Cherepin, V.N. Kolesnik, and M.M. Gumenyuk, Automated Dilatometric Complex, *Instruments and Experimental Technique*, **3**: 147–151 (2010) (in Russian).
78. O.M. Ivasishin, D.G. Savvakin, and M.M. Gumenyak, Dehydrogenation of Titanium-Hydride Powder and Role of This Process in a Sintering Activation, *Metallofiz. Noveishie Tekhnol.*, **33**, No. 7: 899–917 (2011) (in Russian).
79. X.B. Yu, Z. Wu, B.J. Xia, and N.X. Xu, Enhancement of Hydrogen Storage Capacity of Ti–V–Cr–Mn BCC Phase Alloys, *J. Alloys Compd.*, **372**: 272–277 (2004);
https://doi.org/10.1016/j.jallcom.2003.09.153

80. K.N. Young and J. Nei, The Current Status of Hydrogen Storage Alloy Development for Electrochemical Applications, *Materials*, **6**, No. 10: 4574–4608 (2013); https://doi.org/10.3390/ma6104574
81. T.P. Yadav, R.R. Shahi, and O.N. Srivastava, Synthesis, Characterization and Hydrogen Storage Behavior of AB_2 ($ZrFe_2$, $Zr(Fe_{0.75}V_{0.25})_2$, $Zr(Fe_{0.5}V_{0.5})_2$ Type Materials, *Int. J. Hydrogen Energy*, **37**: 3689–3696 (2012); https://doi.org/10.1016/j.ijhydene.2011.04.210
82. F. Stein, M. Palm, and G. Sauthoff, Structure and Stability of Laves Phases. Part I. Critical Assessment of Factors Controlling Laves Phase Stability, *Intermetallics*, **12**, Nos. 7–9 (Spec. Iss.): 713–720 (2004); https://doi.org/10.1016/j.intermet.2004.02.010
83. D.J. Thoma and J.H. Perepezko, A Geometric Analysis of Solubility Ranges in Laves Phases, *J. Alloys Compd.*, **224**: 330–341 (1995); https://doi.org/10.1016/0925-8388(95)01557-4
84. T.V. Pryadko, V.A. Dekhtyarenko, K.M. Khranovs'ka, and H.S. Mohyl'nyi, Influence of the Substitution of Chromium for Manganese on the Structure and Hydrogen-Sorption Properties of $Ti_{47.5}Zr_{30}Mn_{22.5}$ Eutectic Alloy, *Mater. Sci.*, **55**, 854–862 (2020); https://doi.org/10.1007/s11003-020-00379-0
85. O.M. Ivasishin, D.G. Savvakin, M.M. Gumenyak, and O.B. Bondarchuk, Role of Surface Contamination in Titanium PM, *Key Eng. Mater.*, **520**: 121–132 (2012); https://doi.org/10.4028/www.scientific.net/KEM.520.121
86. V.A. Dekhtiarenko, The Influence of Vanadium Addition on Hydrogen Capacity and Absorption–Desorption Kinetics of the Eutectic Ti–Zr–Mn Alloy, *Metallofiz. Noveishie Tekhnol.*, **36**, No. 3: 375–381 (2014) (in Russian); https://doi.org/10.15407/mfint.36.03.0375
87. O.M. Ivasishin, O.B. Bondarchuk, and M.M. Gumenyak, Surface Phenomena During Heating of Titanium Hydride Powder, *Phys. Chem. Solid State*, **12**, No. 4: 900–907 (2011) (in Ukrainian).
88. S. Dong, G. Ma, P. Lei, T. Cheng, D. Savvakin, and O. Ivasishin, Comparative Study on the Densification Process of Different Titanium Powder, *Adv. Powder Technol.*, **32**: 2300–2310 (2021); https://doi.org/10.1016/j.apt.2021.05.009
89. V.G. Ivanchenko, V.A. Dekhtyarenko, T.V. Pryadko, and I.I. Melnyk, Influence of the Laves Phase on Processes of Formation of Hydrides in the Heterophase Alloys of the Ti–Fe–Mn System, *Metallofiz. Noveishie Tekhnol.*, **35**, No. 11: 1465–1473 (2013) (in Russian).
90. V.A. Dekhtyarenko, T.V. Pryadko, D.G. Savvakin, and T.A. Kosorukova, Structure, Phase Composition and Hydrogen Adsorption Properties of Eutectic Alloys of the Ti–Zr–Mn–V System, *Metallofiz. Noveishie Tekhnol.*, **41**, No. 11: 1455–1468 (2019) (in Russian); https://doi.org/10.15407/mfint.41.11.1455

Received 12.03.2024
Final version 05.08.2024

В.А. Дехтяренко[1,2], Т.В. Прядко[1], Т.П. Владімірова[1],
С.В. Максимова[2], Г.Ю. Михайлова[1], В.І. Бондарчук[1]
[1] Інститут металофізики ім. Г.В. Курдюмова НАН України,
бульв. Академіка Вернадського, 36, 03142 Київ, Україна
[2] Інститут електрозварювання ім. Є.О. Патона НАН України,
вул. Казимира Малевича, 11, 03150 Київ, Україна

ВПЛИВ ЛЕГУВАННЯ НА ВОДНЕСОРБЦІЙНІ ВЛАСТИВОСТІ СПЛАВІВ НА ОСНОВІ Ti–Zr–Mn. Ч. 1: Сплави на основі фази Лавеса типу *C*14

Сплави на основі лавесової фази типу *C*14 у системі Ti–Zr–Mn вважаються одними з найперспективніших матеріалів для безпечного зберігання та транспортування водню у зв'язаному стані. Вони мають відносно «м'які» параметри для активації процесів поглинання та виділення водню, невисоку собівартість, а також достатньо високу циклічну стабільність. У статті розглянуто мікроструктуру та фазовий склад вихідних сплавів і кристалічну структуру синтезованих гідридів на їхній основі. Показано можливі шляхи зниження собівартості кінцевого продукту, а також той факт, що зміна способу одержання сплаву не впливає істотно на його воднесорбційні властивості. Також на прикладі розглянутих сплавів показано, що легування сплаву елементом з більшим атомним радіусом, здатним утворювати стійку хімічну сполуку з Гідрогеном, очікувано спричинить збільшення водневої місткості. Це досягається завдяки збільшенню радіуса тетраедричних міжвузловин, де локалізуються атоми Гідрогену під час розчинення, та підвищенню у складі сплаву загальної кількості елементу, здатного взаємодіяти з Гідрогеном.

Ключові слова: фаза Лавеса, інтерметалід, легувальний елемент, тетраедричні міжвузловини, гідрування–дегідрування, воднева місткість.